

# SCIENTIFIC REPORTS



OPEN

## A novel approach to study the structure-property relationships and applications in living systems of modular $\text{Cu}^{2+}$ fluorescent probes

Mengyao She<sup>1,\*</sup>, Zheng Yang<sup>2,\*</sup>, Likai Hao<sup>3</sup>, Zhaohui Wang<sup>1</sup>, Tianyou Luo<sup>1</sup>, Martin Obst<sup>4</sup>, Ping Liu<sup>1</sup>, Yehua Shen<sup>1</sup>, Shengyong Zhang<sup>1</sup> & Jianli Li<sup>1</sup>

Received: 13 April 2016  
Accepted: 07 June 2016  
Published: 03 August 2016

A series of  $\text{Cu}^{2+}$  probe which contains 9 probes have been synthesized and established. All the probes were synthesized using Rhodamine B as the fluorophore, conjugated to various differently substituted cinnamyl aldehyde with C=N Schiff base structural motif as their core moiety. The structure-property relationships of these probes have been investigated. The change of optical properties, caused by different electronic effect and steric effect of the recognition group, has been analyzed systematically. DFT calculation simulation of the Ring-Close and Ring-Open form of all the probes have been employed to illuminate, summarize and confirm these correlations between optical properties and molecular structures. In addition, biological experiment demonstrated that all the probes have a high potential for both sensitive and selective detection, mapping of adsorbed  $\text{Cu}^{2+}$  both *in vivo* and environmental microbial systems. This approach provides a significant strategy for studying structure-property relationships and guiding the synthesis of probes with various optical properties.

Selective recognition and detection of cations by receptors have attracted a significant amount of attention in chemistry, biology, and environmental science<sup>1–4</sup>. Among various detection receptors, fluorescent probe, based ion-induced changes in absorption or fluorescence spectra, appears to be particularly attractive due to their simplicity, high sensitivity, excellent selectivity, and instantaneous response<sup>5–7</sup>. However, properties of a fluorescent probe depend strongly on the binding properties of the target cation and the recognizing site in probe molecular<sup>8,9</sup>. Therefore, the binding properties and the geometrical configuration of the coordination sites in the corresponding probes are the most important parameters to consider during design and synthesis fluorescent probes. A commonly strategy is to attach a ligand in fluorophore to form the target recognizing site in the design of fluorescent probes<sup>10–12</sup>. High sensitivity and selectivity are fundamental goals and core design principles for an excellent probe. Though a large amount of researches had reported in the past decades, these researches did not mention electronic and steric effects that can regulate the performance in the recognition process<sup>13–16</sup>.

Copper, as the third most abundant essential trace element in human body, plays a crucial role for a broad range of biological processes<sup>17–20</sup>. However, copper excess cause toxicity to most living organisms, and copper release can eventually lead to serious environmental contamination<sup>21–23</sup>. Therefore, a convenient and rapid method for the detection of copper became increasingly important in biological and environmental concerns. Though chelating of  $\text{Cu}^{2+}$  with chemo sensors is well known to induce intrinsic fluorescence quenching due to the paramagnetic nature of  $\text{Cu}^{2+}$ <sup>24</sup>, hundreds of fluorescent probes have been developed for varying purposes within the last few decades<sup>25–27</sup>. Systematic studies of these effects thus have expected to get great significance for the further development of  $\text{Cu}^{2+}$  fluorescent probes. Evermore, selection of an adequate probe for CLSM studies in bio-, geo-, and environmental sciences became more and more challenging<sup>28</sup>.

<sup>1</sup>Ministry of Education Key Laboratory of Synthetic and Natural Functional Molecule Chemistry, College of Chemistry & Materials Science, Northwest University, Xi'an, Shaanxi 710127, P. R. China. <sup>2</sup>College of Chemistry and Chemical Engineering, Xi'an University of Science and Technology, Xi'an, Shaanxi 710054, P. R. China. <sup>3</sup>Center for Applied Geoscience, Institute for Geoscience, Eberhard Karls University Tuebingen, Hoelderlinstr. 12, Tuebingen 72074, Germany. <sup>4</sup>Bayreuth Center for Ecology and Environmental Research (BayCEER), University of Bayreuth, Dr.-Hans-Frisch-Str. 1-3, Bayreuth 95448, Germany. \*These authors contributed equally to this work. Correspondence and requests for materials should be addressed to J.L. (email: lijianli@nwu.edu.cn)

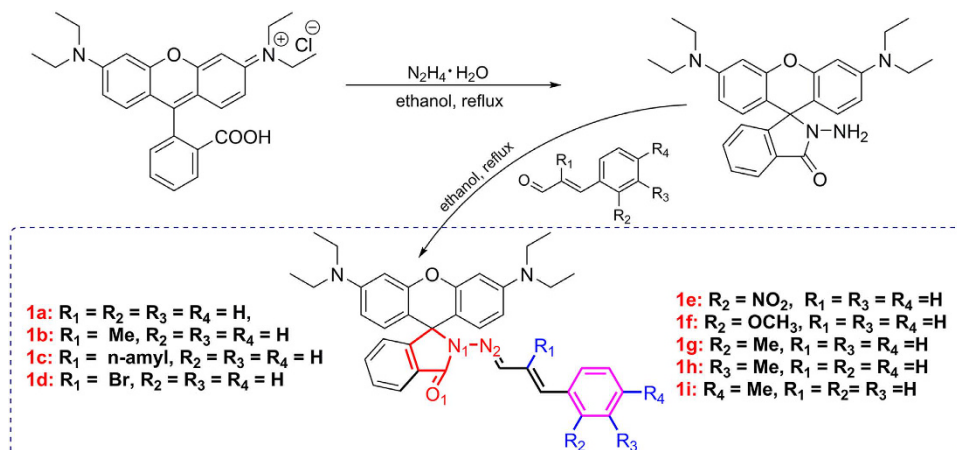


**Figure 1.** Synthesis route and molecular structure of probes 1a-1i.

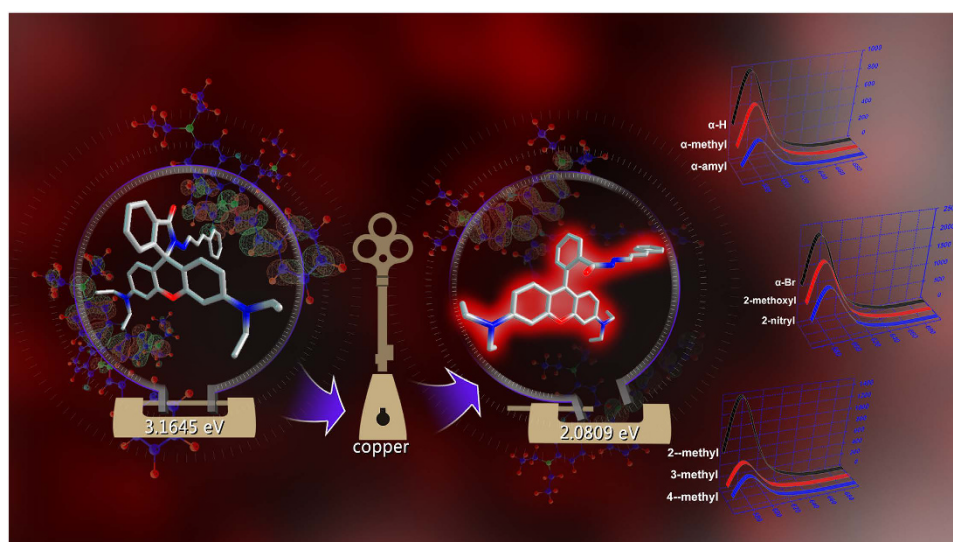


**Figure 2.** Schematic of the strategy for studying structure-property relationships of 9 modular  $Cu^{2+}$  fluorescent probes.

In order to investigate the effect of structure on performance for a probe, we synthesized and established a series of  $Cu^{2+}$  probe which contains 9 probes 1a-1i based on our previous work (Fig. 1)<sup>29</sup>. Each of them is synthesized using rhodamine B as the fluorophore, conjugated to various differently substituted cinnamyl aldehyde with C=N Schiff base structural motif as its core segment. These probes show superior stable optical properties for the detection of  $Cu^{2+}$  which are not affect by fluorescence quenching. All these probes are synthesized easily under chemically mild conditions with a high yield (>80%) through a two-step reaction via Rhodamine B with substituted cinnamyl aldehyde. To our surprise, all probes showed different absorption and fluorescence responsive intensity to  $Cu^{2+}$ .

In this work, we focused on the structure-property relationships of this probe model, investigated the change of optical properties caused by different electronic effect and steric effect of the recognition group, and also employed DFT calculation simulate the Ring-Close and Ring-Open form of all the probes (Fig. 2). Comprehensive analyses on the regulatory effects of substituent group about this probe model have been elaborated using frontier molecular orbital theory, NBO charge population and Fukui functional analysis.

## Results and Discussion

**UV-vis properties.** Binding affinities of each probe toward varies metal ions, namely the chloride salts of  $Li^+$ ,  $Na^+$ ,  $K^+$ ,  $Ba^{2+}$ ,  $Ca^{2+}$ ,  $Cd^{2+}$ ,  $Mg^{2+}$ ,  $Co^{2+}$ ,  $Mn^{2+}$ ,  $Zn^{2+}$ ,  $Pb^{2+}$ ,  $Ni^{2+}$ ,  $Fe^{2+}$ ,  $Hg^{2+}$ ,  $Fe^{3+}$ ,  $Al^{3+}$ ,  $Cr^{3+}$ ,  $Cu^{2+}$  and the nitrate salt of  $Ag^+$  were evaluated by UV-vis spectroscopy. Upon addition of the respective metal ions, the absorption spectrum of the individual probes changed in different manners as shown in Figure S9. However, all tested metal ions but  $Cu^{2+}$  showed only minor spectral or color changes. Similar responses were observed when  $Cu^{2+}$  ions were added to the probe solutions in the presence of other metal ions. The absorption spectrum of probe 1a-1i

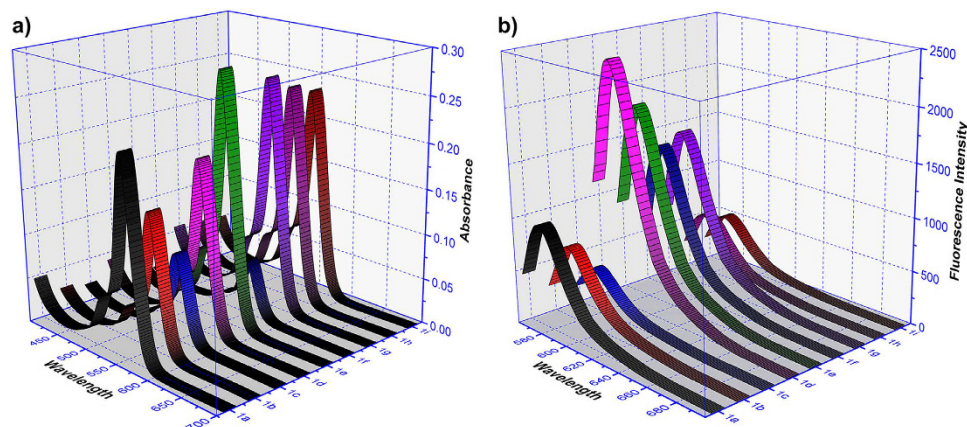


**Figure 3.** Absorbance and fluorescence intensities of probes **1a-1i** ( $10\ \mu\text{M}$ ) +  $\text{Cu}^{2+}$  ( $50\ \mu\text{M}$ ) in ethanol-PBS (5/5, v/v, pH 7.4), (a) Absorbance: maximum absorption at 556 nm; (b) fluorescence intensities:  $\lambda_{\text{ex}} = 550\ \text{nm}$ ,  $\lambda_{\text{em}} = 576\ \text{nm}$ .

exhibited a broad band at 556 nm at room temperature in the PBS buffer solution (pH = 7.4, 50% (v/v) ethanol). Since the closed form of rhodamine did not show an intense absorption band in the visible region<sup>30</sup>, this result suggested that probe  $\text{Cu}^{2+}$  complexes were not present in the form of closed spirolactone, but in an opened configuration at neutral pH. Furthermore, the absorption response all individual probes toward  $\text{Cu}^{2+}$  showed linear relationships in the range 0–50.0  $\mu\text{M}$  of  $\text{Cu}^{2+}$  (all the graphs are showed in Supplementary Information).

More importantly, the UV absorbance of these probes were shown to be adjusted by the different substituent groups. As shown in (Fig. 3a), the comparison of probe **1a**, **1b**, **1c** indicates that with a volume increases of  $\mathbf{R}_1$ , the strength of UV absorbance decreases; the reasons for this phenomenon may be caused by the increase of steric hindrance effects that obstruct the combination of probe with  $\text{Cu}^{2+}$ . In other words,  $\mathbf{R}_1$  plays a negative, volume-dependent role in the detection of  $\text{Cu}^{2+}$ . When other heavy elements used as substituent at position  $\mathbf{R}_1$  instead, the UV absorption spectrum in presence of  $\text{Cu}^{2+}$  showed a strong absorption band. In this study, we used Br as a substituent for instance. Moreover, we recognized visually that electronegative groups in the specific recognition unit of probe had a positive effect on the UV absorbance whereas electron-donating groups have a negative effect (probe **1e**:  $\mathbf{R}_1 = \text{NO}_2$ , probe **1f**:  $\mathbf{R}_1 = \text{OCH}_3$ ). In addition, the absorbance of the probe +  $\text{Cu}^{2+}$  complexes were reduced gradually (**1g** > **1h** > **1i**), when methyl was introduced into different positions of benzene ring, whereas in ortho-, meta-, para-position it had scarcely any effect on the UV absorbance response in this series of probes.

**Fluorescence properties.** The fluorescence properties of the probes and their respective responses to  $\text{Cu}^{2+}$  was evaluated in ethanol-PBS (5/5, v/v, pH 7.4) solution. The remarkable orange fluorescence emission of our probes increase that is induced by  $\text{Cu}^{2+}$  can interpreted as the opening of the spiral ring at appropriate pH; the emission band of this probe series appeared at 576 nm. The changes of **1a-1i** ( $10\ \mu\text{M}$ ) upon addition of  $\text{Cu}^{2+}$  (0–5.0 equiv.) have been studied (Figure S9). Fluorescence titration spectra of **1a-1i** with  $\text{Cu}^{2+}$  from 0  $\mu\text{M}$  to 50  $\mu\text{M}$  showed that these spectroscopic responses increased with increasing concentration of  $\text{Cu}^{2+}$  for each probe in this series. We also performed competition experiments with metal ions other than  $\text{Cu}^{2+}$  under the same conditions as for the absorbance study. The result revealed that this series of probes has significant anti-jamming capabilities in the presence of 5.0 equiv. of other ions (Figure S5). Furthermore, concentrations of  $\text{Cu}^{2+}$  and fluorescence intensities have a good linear relationship as shown in Figure S6. The coordination also shown to be a reversible process. When excess ethylenediamine was added to the colored solution of the complex, the fluorescence disappeared and the pink solution turned back to colorless owing to the de-coordination of  $\text{Cu}^{2+}$ . Thus, **1a-1i** can be classified as a conditional reversible probe for  $\text{Cu}^{2+}$ .

As show in (Fig. 3b), fluorescence intensity of probe **1a-1c** was reduced by increasing steric hindrance of substituent group  $\mathbf{R}_1$ . In addition, heavy elements substituting for  $\mathbf{R}_1$  (e.g. Br) enhanced the fluorescence response significantly. For comparison, we have synthesized a congeneric probe **1j** which is substituted by Cl at the same position of Br and exhibited a lower fluorescence intensity than that of **1d**. Similarly, we introduced  $-\text{NO}_2$  and  $-\text{OCH}_3$  substituents to the recognition unit of the molecule to analyze the relationship between fluorescence intensity and electronic effects. The result suggested that electron-drawing groups promote fluorescence enhancement to a higher extent as compared to electron-donating groups. Substitutions in the ortho-position of the benzene ring increased the fluorescence intensity, whereas this effect was not observed when the substitution was inserted in meta- or para-position.

**Theoretical calculation analysis.** To better understand the structure-property relationships of these 9 probes, the mode of ring-close and ring-open were studied by DFT<sup>31</sup> calculations, all the calculations were performed with B3LYP functional with a combination of basis of double- $\zeta$  quality consisting of 6-31G\*\* for C, H elements and 6-31+G\* for N, O, Br elements on Gaussian 09 Program<sup>32</sup>. (Full citations are given in supporting information). The optimized structures were confirmed to be local minimums due to the non-existence of imaginary frequency. The environmental effect was included via PCM model with ethanol as the solvent molecule.

No.	Ring-close form (C)	Ring-open form (O)	$\Delta E$ (Kcal/mol)
	Total Energy (a.u.)	Total Energy (a.u.)	
1	-1802.3177	-1802.2962	13.5098
2	-1841.6321	-1841.6095	14.2351
3	-1998.8926	-1998.8673	15.8898
4	-4373.1169	-4373.0969	12.5093
5	-2006.8251	-2006.8018	14.6411
6	-1916.8454	-1916.8230	14.0357
7	-1841.6329	-1841.6110	13.7240
8	-1841.6377	-1841.6160	13.6003
9	-1841.6383	-1841.6162	13.8344

**Table 1.** The calculated energy(E) of all structures.

As show in Table 1, all the Ring-Open forms possesses higher energy than that of Ring-Close form over 12 Kcal/mol. These results indicated that these probes prefer to present in a lactam form without environmental disturbance. Especially, probe **1a-1c** show gradualness energy increase, which may be attributed to the block transition process by the growing steric hindrance. Extraordinary for probe **1d**, the exist of heavy atom Br could promote the equalization of electronic cloud distribution and reduce energy accordingly, and the energy required for the formation of Ring-Open structure is less than any other probe, which indicated that probe **1d** may show a better optical property because of its easy changed structure. The molecule energy seems to be insensitive to the Push-pull electronic effect and spatial effect on the benzene ring of recognition group.

The HOMO-LUMO orbital energies and the spatial distributions for these probes were determined; the spatial distributions HOMO and LUMO were displayed in Fig. 4. In the Ring-Close form, all HOMOs were distributed to xanthene moiety and LUMOs were located on the recognition part. The distribution was exactly the opposite in the Ring-Open form. It's obvious that all the Ring-Open structures have higher HOMO energy and lower LUMO energy except probe **1e**. The LUMO energy of probe **1e** showed an abnormal reduction from other probes, which may due to the evenly distributed electron density caused by the strong electrophilic effect of NO<sub>2</sub>.

The results of NBO analysis<sup>33</sup> demonstrate the polarization of Charge distribution (Fig. 5), the electron was flowing from xanthene moiety to the recognized moiety during the process of transform, the charge is which was consistent with reported literature. The larger density of electron cloud represents the higher electron donating ability.

On the other hand,  $f_{(r)}$  has been successfully used to describe the reactivity concerning electrophilic attack<sup>34</sup>, CuCl<sub>2</sub> attack in this model of probe. The condensed Fukui function of individual atom is obtained from NBO analysis. As show in Fig. 5 the 3D representation of the  $f_{(r)}$  clearly demonstrates that the region around carbonyl O atom and hydrazide N atom possesses higher reactivity than other parts of the Ring-Open form and there is no obvious electrophilic site in the recognized moiety of Ring-Close form. These data illustrate that all the probes have the tendency to be opened rather than closed under the entrainment and coordination of Cu<sup>2+</sup>.

**CLSM bioimaging applications.** These probes were selected for Cu<sup>2+</sup>-localization studies in microbial cell-extracellular polymeric substances (EPS)-mineral aggregates. The photosynthetic Fe(II)-oxidizing *Rhodobacter* sp. strain SW2 was selected as an model organism because SW2 is known to form such aggregates<sup>35</sup> and for being highly resistant to heavy metals during its Fe(II) oxidization<sup>36</sup>. It was incubated under permanent illumination in fresh water mineral medium for 1 week. The resulting suspension of aggregates that consisted of microbial cells, extracellular polymers and Fe(III)-minerals was equilibrated with 50 μM of CuCl<sub>2</sub> for 30 min. Probe **1a-1i** (50 μM), SYTO 9 green fluorescent nucleic acid stain (1:500) and polysaccharide-specific Wheat germ agglutinin, ALEXA FLUOR 633 conjugate (1:200)<sup>28,29</sup> were applied to visualize the distribution of Cu<sup>2+</sup>, bacterial cells and EPS respectively. The CLSM images show that probe **1a-1i** was able to detect Cu<sup>2+</sup> in the aqueous microbial cell-EPS-mineral aggregates. The results furthermore indicate that Cu<sup>2+</sup> is collocated with the bacterial cells and with the free, cloud-like EPS, suggesting that the organic surfaces provide binding sites for Cu<sup>2+</sup>, even though the detailed spatial distribution of Cu<sup>2+</sup> on subcellular level and microbial sorption mechanism still remain unclear and need to be analyzed by higher resolution analytical microscopy approaches (Fig. 6). In summary, probe **1a-1i** can be used to label Cu<sup>2+</sup>-biosorption in microbial cell-EPS-mineral aggregates and bio-films. Since their fluorescence spectra are compatible for the combination with commercial available DNA- and polysaccharide-specific fluorescent dyes, they further provide the possibility to explore the correlation between Cu<sup>2+</sup> and organic components in this system on the single cell level under natural and hydrated conditions. Our approach also provides a successful case wherein it is shown how to design, synthesize and improve other metal fluorescent probes with high sensitivity and selectivity. Finally, our attempt also revealed that the library-based strategy<sup>37</sup> for imaging-based fluorescence screening is a powerful tool to select the most appropriate fluorescent metal probes for CLSM studies.

**Living cells bioimaging applications.** Next, we proceeded to investigate the utility of probe **1a-1i** in intracellular imaging with L929 to examine whether it can work in biological systems, the distribution of the probe within the cells was observed by laser scanning confocal microscopy following excitation at 543 nm. As show in Fig. 7, all the probes can permeate cellular membrane due to the molecule as well hydrophobicity, following

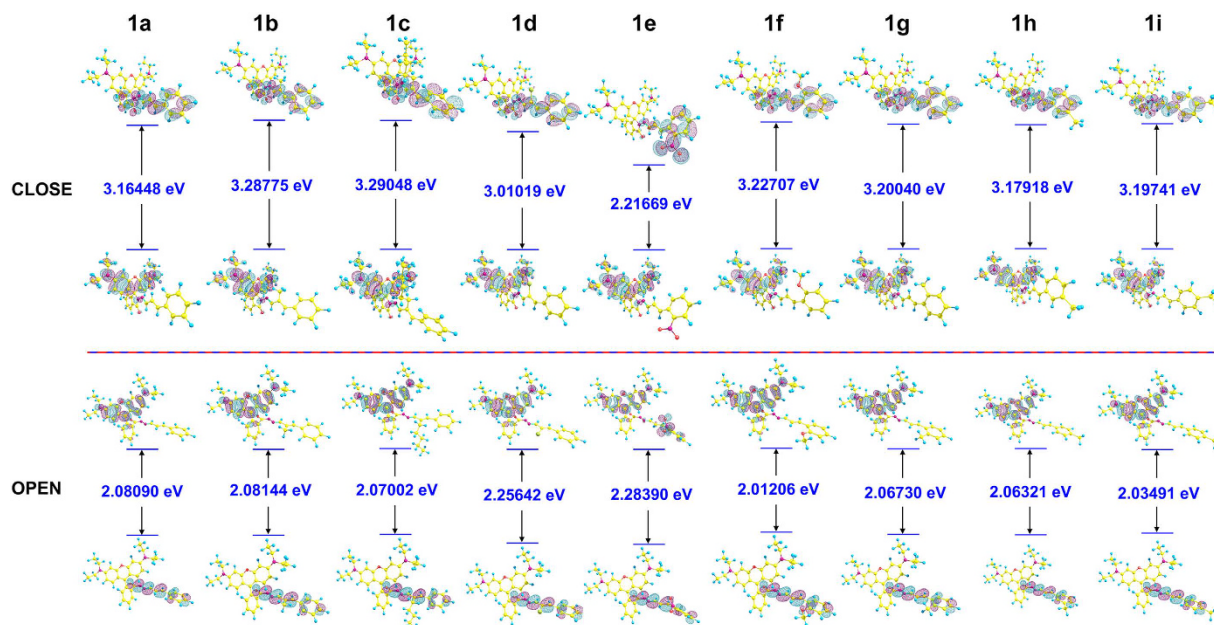


**Figure 4.** The HOMO-LUMO Gaps of probe 1a-1i.

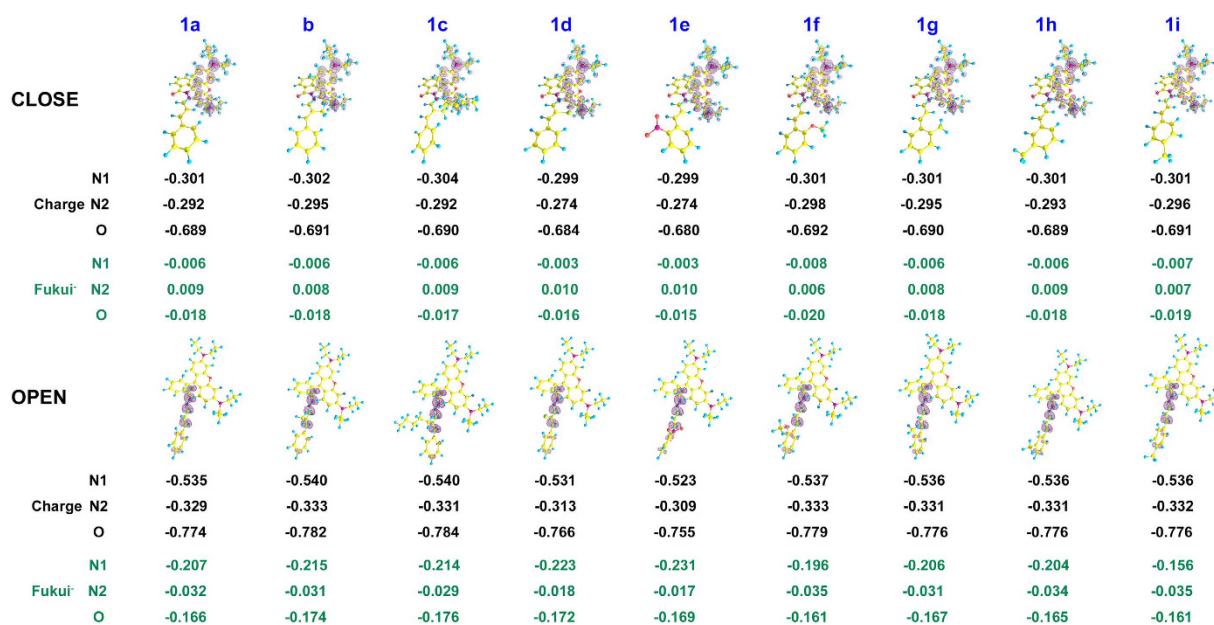


**Figure 5.** NBO charge, 3D representation of the Fukui function  $f_{(r)}^-$  of the iso-value of 0.003 a.u. (positive in red color and negative in green color) and the D-value condensed Fukui function  $f_{(r)}^-$  of O, N<sub>1</sub> and N<sub>2</sub>.

addition of exogenous Cu<sup>2+</sup>, show relatively obvious intracellular fluorescence with excitation. Bright-field transmission measurements after the probe incubation confirm that the cells are viable. The overlay of fluorescence and bright-field images revealed that the fluorescence signals were localized in the perinuclear region of the cytosol, indicating the subcellular distribution of Cu<sup>2+</sup> which was internalized into the living cells from the growth medium. We anticipate that these probes will be of great benefit for biomedical researchers investigating the effects of Cu<sup>2+</sup> in biological systems.

## Methods

**Materials and Methods.** All the reagent grade chemicals consumed in this work were procured from commercial sources and used as received. Cu<sup>2+</sup> stock solution is prepared to be 200 μmol/L with ethanol using CuCl<sub>2</sub> as the source, and probe 1a-1i stock solution (50 ml) were prepared to be 200 μmol/L with ethanol and solubilized by little acetone (0.1 ml). The solutions of metal ions were prepared in ethanol for the selectivity and competitive

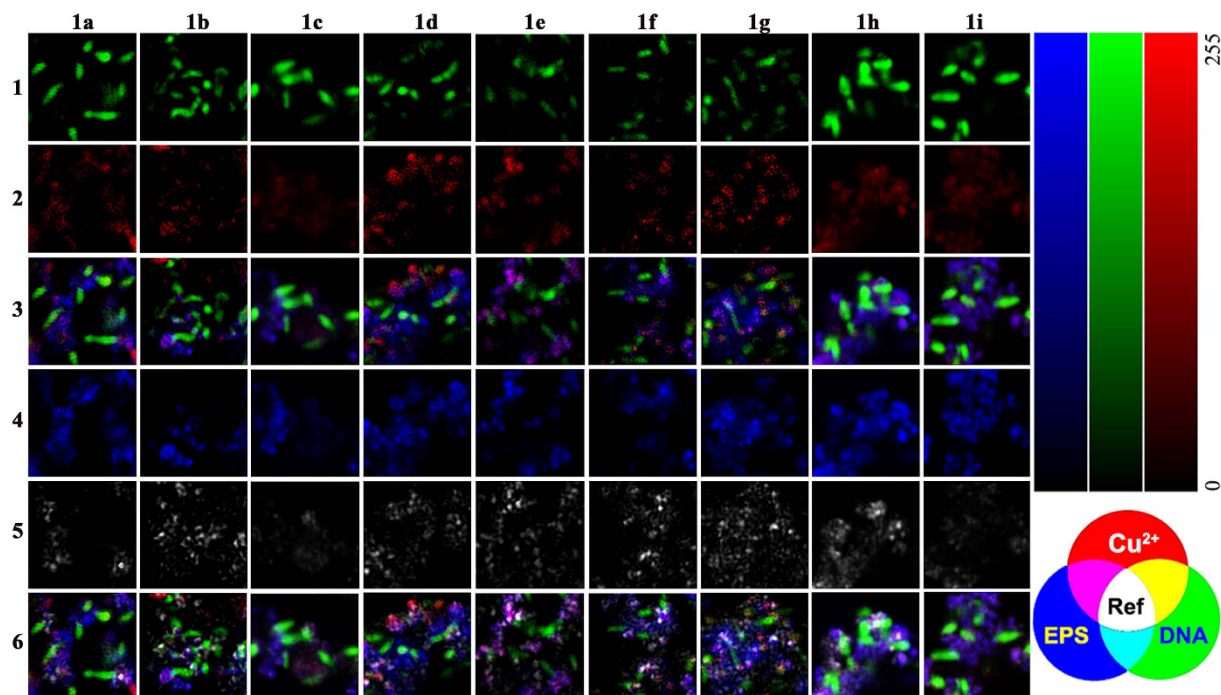


**Figure 6.** Single cell scale maps showing the sorption of  $\text{Cu}^{2+}$  to cell-EPS-mineral aggregates formed by Fe(II)-oxidizing *Rhodobacter* sp. strain SW2 incubated with  $50 \mu\text{M}$   $\text{CuCl}_2$  for 1 h at  $25^\circ\text{C}$ . The aggregate was simultaneously incubated with  $50 \mu\text{M}$  of probes 1a-1i (2) and 20%  $\text{C}_2\text{H}_5\text{OH}$ , fluorescent nucleic acid stain (1) and lectin conjugate (4) for 1 h at  $25^\circ\text{C}$ , minerals of biogenic origin were visualized employing their reflection signal (5) ( $\lambda_{\text{ex}} = 488 \text{ nm}, 561 \text{ nm}, 635 \text{ nm}$ ). The overlay image of (1) (2) and (4) is shown in (3); the overlay image of all four signals is shown in (6). Brighter colour indicates a higher metal concentration.

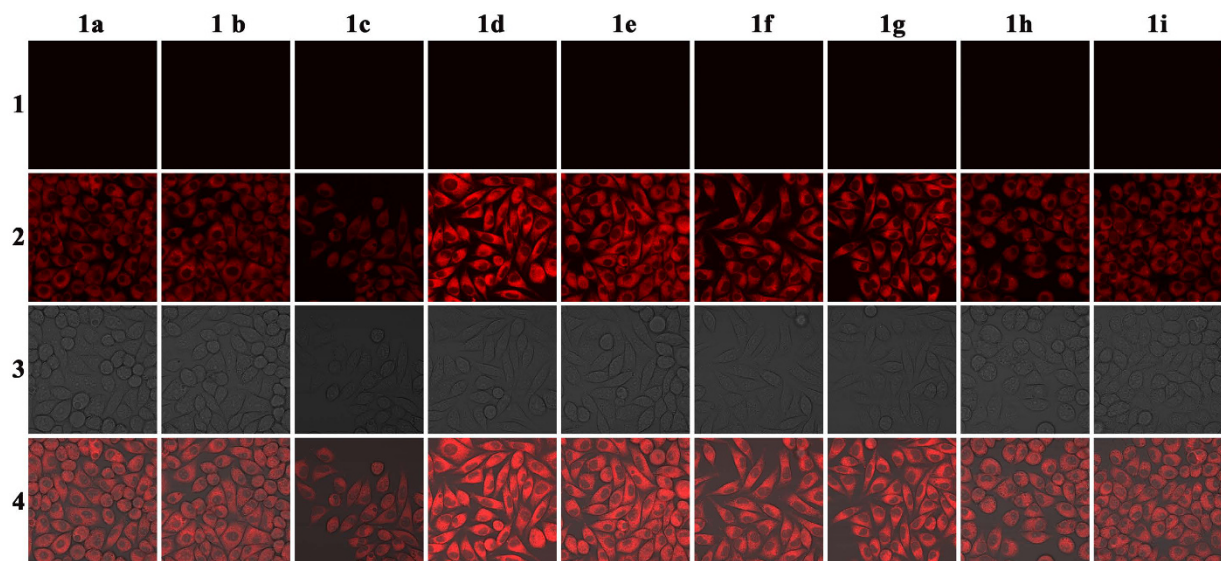


**Figure 7.** Fluorescent images of L929 cells incubated with  $10 \mu\text{M}$  probes for 30 min (1) and then further incubated with  $50 \mu\text{M}$   $\text{Cu}^{2+}$  for 30 min (2). (3) Bright field image of cells. The overlay image of (2) and (3) is shown in (4) ( $\lambda_{\text{ex}} = 543 \text{ nm}$ ).

study with chloride salts of  $\text{Li}^+$ ,  $\text{Na}^+$ ,  $\text{K}^+$ ,  $\text{Ba}^{2+}$ ,  $\text{Ca}^{2+}$ ,  $\text{Cd}^{2+}$ ,  $\text{Mg}^{2+}$ ,  $\text{Co}^{2+}$ ,  $\text{Mn}^{2+}$ ,  $\text{Zn}^{2+}$ ,  $\text{Pb}^{2+}$ ,  $\text{Ni}^{2+}$ ,  $\text{Fe}^{2+}$ ,  $\text{Hg}^{2+}$ ,  $\text{Fe}^{3+}$ ,  $\text{Al}^{3+}$ ,  $\text{Cr}^{3+}$ ,  $\text{Cu}^{2+}$  and the nitrate salt of  $\text{Ag}^+$ .

To a 10 mL volumetric tube, different concentration of  $\text{Cu}^{2+}$ , 5.0 mL PBS and 0.50 mL of  $200 \mu\text{M}$  probes were added. The mixtures were diluted to 10 mL with ethanol. Then, 3.0 mL of each solution were transferred to a 1 cm cuvette. The absorbance was recorded at 556 nm and the fluorescence intensity was recorded at 576 nm. The

excitation and emission wavelength bandpasses were both set as 5.0 nm and the excitation wavelength was set at 550 nm.

A Beijing TAIKE XT-4 microscopy melting point apparatus was used to measure the melting points of the compounds. Mass spectrometry was performed on a BRUKER micrOTOF-Q II ESI-Q-TOF LC/MS/MS Spectroscopy. NMR spectra were recorded on a VARIAN INOVA-400 spectrometer, using TMS (TMS trimethylsilyl) as an internal standard. The absorbance spectra were recorded on a SHIMADZU UV-1700 spectrophotometer. A HITACHI F-4500 FL spectrophotometer employed to record the fluorescence spectra. A VARIO EL III analyzer was used for performing the elemental analyses. Samples for mapping Cu<sup>2+</sup> sorption to cell-mineral aggregates of Fe(II)-oxidizing bacteria were prepared under anoxic conditions in a glovebox under N<sub>2</sub> atmosphere. The samples were analyzed using an upright confocal laser scanning microscope (LEICA SPE, Wetzlar, Germany), equipped with 4 lasers (405 nm, 488 nm, 561 nm, 635 nm) and a 63x water immersion objective (ACS APO 63x, NA = 1.15).

## Conclusions

In summary, we have synthesized and evaluated a series of Cu<sup>2+</sup> probe which contains 9 probes, all the probes are based on the core segment of C=N Schiff base structural motif. This study revealed the relation between the structure and the optical properties of nine probes focusing on the influence of various substituents and provided a significant strategy for studying structure-property relationships which were illuminated, summarized and confirmed by DFT calculation simulation on the Ring-Close and Ring-Open form of this modular Schiff base Cu<sup>2+</sup> fluorescent probes. We expect that these results of our research would help to guide the synthesis of high performance metal fluorescence probes with various properties. On the other hand, all the probes could permeate cellular membrane to investigating the effects of Cu<sup>2+</sup> in living cells. Furthermore, CLSM experiments suggested that all the probes would be a powerful tool for sensitive and selective detection and mapping of Cu<sup>2+</sup> adsorbed in environmental microbial systems.

## References

1. Qian, X. & Xu, Z. Fluorescence imaging of metal ions implicated in diseases. *Chemical Society Reviews* **44**, 4487–4493 (2015).
2. Zhang, Z. *et al.* Simultaneous Quantification of Hg<sup>2+</sup> and MeHg<sup>+</sup> in Aqueous Media with a Single Fluorescent Probe by Multiplexing in the Time Domain. *Analytical Chemistry* **86**, 11919–11924 (2014).
3. Lee, M. H., Kim, J. S. & Sessler, J. L. Small molecule-based ratiometric fluorescence probes for cations, anions, and biomolecules. *Chemical Society Reviews* **44**, 4185–4191 (2015).
4. Yin, J., Hu, Y. & Yoon, J. Fluorescent probes and bioimaging: alkali metals, alkaline earth metals and pH. *Chemical Society Reviews* **44**, 4619–4644 (2015).
5. Aich, K. *et al.* Cd<sup>2+</sup> Triggered the FRET “ON”: A New Molecular Switch for the Ratiometric Detection of Cd<sup>2+</sup> with Live-Cell Imaging and Bound X-ray Structure. *Inorganic Chemistry* **54**, 7309–7315 (2015).
6. Zhu, H., Fan, J., Wang, B. & Peng, X. Fluorescent, MRI, and colorimetric chemical sensors for the first-row d-block metal ions. *Chemical Society Reviews* **44**, 4337–4366 (2015).
7. Han, Y., Ding, C., Zhou, J. & Tian, Y. Single Probe for Imaging and Biosensing of pH, Cu<sup>2+</sup> Ions, and pH/Cu<sup>2+</sup> in Live Cells with Ratiometric Fluorescence Signals. *Analytical Chemistry* **87**, 5333–5339 (2015).
8. Kuo, S. *et al.* Dual Colorimetric and Fluorescent Sensor Based On Semiconducting Polymer Dots for Ratiometric Detection of Lead Ions in Living Cells. *Analytical Chemistry* **87**, 4765–4771 (2015).
9. Zhang, H. *et al.* Solid-Phase Synthesis of Highly Fluorescent Nitrogen-Doped Carbon Dots for Sensitive and Selective Probing Ferric Ions in Living Cells. *Analytical Chemistry* **86**, 9846–9852 (2014).
10. Dong, B. *et al.* Dual Site-Controlled and Lysosome-Targeted Intramolecular Charge Transfer–Photoinduced Electron Transfer–Fluorescence Resonance Energy Transfer Fluorescent Probe for Monitoring pH Changes in Living Cells. *Analytical Chemistry* **88**, 4085–4091 (2016).
11. Chen, H., Tang, Y., Ren, M. & Lin, W. Single near-infrared fluorescent probe with high- and low-sensitivity sites for sensing different concentration ranges of biological thiols with distinct modes of fluorescence signals. *Chemical Science* **7**, 1896–1903 (2016).
12. Goswami, S. *et al.* Nanomolar Detection of Hypochlorite by a Rhodamine-Based Chiral Hydrazide in Absolute Aqueous Media: Application in Tap Water Analysis with Live-Cell Imaging. *Analytical Chemistry* **86**, 6315–6322 (2014).
13. Lu, X. *et al.* A multi-functional probe to discriminate Lys, Arg, His, Cys, Hcy and GSH from common amino acids. *Chemical Communications* **51**, 1498–1501 (2015).
14. Sun, Y. *et al.* A Mitochondria-Targetable Fluorescent Probe for Dual-Channel NO Imaging Assisted by Intracellular Cysteine and Glutathione. *Journal of the American Chemical Society* **136**, 12520–12523 (2014).
15. Yokoi, H., Hiroto, S. & Shinokubo, H. Synthesis of Diazo-Bridged BODIPY Dimer and Tetramer by Oxidative Coupling of  $\beta$ -Amino-Substituted BODIPYs. *Organic Letters* **16**, 3004–3007 (2014).
16. Yapici, N. B. *et al.* Highly Stable and Sensitive Fluorescent Probes (LysoProbes) for Lysosomal Labeling and Tracking. *Scientific Reports* **5**, 8576 (2015).
17. Fan, C. *et al.* A novel copper complex of salicylaldehyde pyrazole hydrazone induces apoptosis through up-regulating integrin  $\beta$ 4 in H322 lung carcinoma cells. *European Journal of Medicinal Chemistry* **45**, 1438–1446 (2010).
18. Zhang, B. *et al.* A sensitive fluorescent probe for Cu<sup>2+</sup> based on rhodamine B derivatives and its application to drinking water examination and living cells imaging. *Sensors and Actuators B: Chemical* **225**, 579–585 (2016).
19. Zong, L., Song, Y., Li, Q. & Li, Z. A. “turn-on” fluorescence probe towards copper ions based on core-substituted naphthalene diimide. *Sensors and Actuators B: Chemical* **226**, 239–244 (2016).
20. Cotruvo, J. J. A., Aron, A. T., Ramos-Torres, K. M. & Chang, C. J. Synthetic fluorescent probes for studying copper in biological systems. *Chemical Society Reviews* **44**, 4400–4414 (2015).
21. Taki, M., Iyoshi, S., Ojida, A., Hamachi, I. & Yamamoto, Y. Development of Highly Sensitive Fluorescent Probes for Detection of Intracellular Copper(I) in Living Systems. *Journal of the American Chemical Society* **132**, 5938–5939 (2010).
22. Crichton, R. R., Dexter, D. T. & Ward, R. J. Metal based neurodegenerative diseases—From molecular mechanisms to therapeutic strategies. *Coordination Chemistry Reviews* **252**, 1189–1199 (2008).
23. Garenaux, A. & Dozois, C. M. Metals: Ironing out copper toxicity. *Nat Chem Biol* **8**, 680–681 (2012).
24. Yao, J. *et al.* Efficient Ratiometric Fluorescence Probe Based on Dual-Emission Quantum Dots Hybrid for On-Site Determination of Copper Ions. *Analytical Chemistry* **85**, 6461–6468 (2013).
25. Wu, P. *et al.* Cadmium-Based Metal–Organic Framework as a Highly Selective and Sensitive Ratiometric Luminescent Sensor for Mercury(II). *Inorganic Chemistry* **54**, 11046–11048 (2015).
26. Li, J. *et al.* Fluorescence turn-on detection of mercury ions based on the controlled adsorption of a perylene probe onto the gold nanoparticles. *The Analyst* **141**, 346–351 (2016).

27. Yang, Y., Zhao, Q., Feng, W. & Li, F. Luminescent Chemodosimeters for Bioimaging. *Chemical Reviews* **113**, 192–270 (2012).
28. Hao, L., Li, J., Kappler, A. & Obst, M. Mapping of Heavy Metal Ion Sorption to Cell-Extracellular Polymeric Substance-Mineral Aggregates by Using Metal-Selective Fluorescent Probes and Confocal Laser Scanning Microscopy. *Applied and Environmental Microbiology* **79**, 6524–6534 (2013).
29. Yang, Z. *et al.* Highly sensitive and selective rhodamine Schiff base “off-on” chemosensors for Cu<sup>2+</sup> imaging in living cells. *Sensors and Actuators B: Chemical* **176**, 482–487 (2013).
30. Hirayama, T., Okuda, K. & Nagasawa, H. A highly selective turn-on fluorescent probe for iron(II) to visualize labile iron in living cells. *Chemical Science* **4**, 1250–1256 (2013).
31. Becke, A. D. Density-functional thermochemistry. III. The role of exact exchange. *Journal of Chemical Physics* **98**, 5648 (1993).
32. Frisch, M. J. *et al.* GAUSSIAN 09, Revision A.02, Gaussian, Inc., Wallingford, CT, 2009.
33. Yin, B., Huang, Y., Wang, G. & Wang, Y. Combined DFT and NBO study on the electronic basis of Si–N-β-donor bond. *Journal of Molecular Modeling* **16**, 437–446 (2009).
34. She, M. *et al.* An efficiently cobalt-catalyzed carbonylative approach to phenylacetic acid derivatives. *Tetrahedron* **69**, 7264–7268 (2013).
35. Hegler, F., Posth, N. R., Jiang, J. & Kappler, A. Physiology of phototrophic iron(II)-oxidizing bacteria: implications for modern and ancient environments. *Fems Microbiology Ecology* **66**, 250–260 (2008).
36. Hohmann, C., Winkler, E., Morin, G. & Kappler, A. Anaerobic Fe(II)-Oxidizing Bacteria Show As Resistance and Immobilize As during Fe(III) Mineral Precipitation. *Environmental Science & Technology* **44**, 94–101 (2009).
37. Kang, N., Ha, H., Yun, S., Yu, Y. & Chang, Y. Diversity-driven chemical probe development for biomolecules: beyond hypothesis-driven approach. *Chemical Society Reviews* **40**, 3613–3626 (2011).

## Acknowledgements

We thank E. D. Swanner, P. Ingino and W. Wu (University of Tuebingen) for their support. This work was supported by the National Natural Science Foundation of China (No. 21572177; 21272184 and J1210057), the Shaanxi Provincial Natural Science Fund Project (No. 2015JZ003), the Xi'an City Science and Technology Project (No. CXY1511(3)), the Northwest University Science Foundation for Postgraduate Students (No. YZZ14052), the Chinese National Innovation Experiment Program for University Students (No. 201510697004) and the Emmy-Noether fellowship program of the DFG to M.O. (OB 362/1-1) for financial support.

## Author Contributions

M.S. designed the study, theoretical calculation analysis and wrote the manuscript. Z.Y. performed the probes characterization, cell assays and edited the manuscript. Z.W. and T.L. did the synthesis of these fluorescent probes. L.H. and M.O. performed the CLSM bioimaging applications. P.L. and Y.S. edited the manuscript, S.Z. and J.L. supervised the project. All authors reviewed the manuscript.

## Additional Information

**Supplementary information** accompanies this paper at <http://www.nature.com/srep>

**Competing financial interests:** The authors declare no competing financial interests.

**How to cite this article:** She, M. *et al.* A novel approach to study the structure-property relationships and applications in living systems of modular Cu<sup>2+</sup> fluorescent probes. *Sci. Rep.* **6**, 28972; doi: 10.1038/srep28972 (2016).



This work is licensed under a Creative Commons Attribution 4.0 International License. The images or other third party material in this article are included in the article's Creative Commons license, unless indicated otherwise in the credit line; if the material is not included under the Creative Commons license, users will need to obtain permission from the license holder to reproduce the material. To view a copy of this license, visit <http://creativecommons.org/licenses/by/4.0/>